Urban heat island intensity and its relationship with ozone in Joint Urban 2003 campaign

Xiao-Ming Hu[1], Petra M. Klein[1,2], Ming Xue[1,2]

Xiao-Ming Hu, Center for Analysis and Prediction of Storms, University of Oklahoma, National Weather Center, 120 David L. Boren Blvd, Suite 2500, Norman, OK 73072-7309, USA. (xhu@ou.edu)

[1]Center for Analysis and Prediction of Storms, University of Oklahoma, Norman, OK, USA

[2]School of Meteorology, University of Oklahoma, Norman, OK, USA

Abstract. WRF/Chem-UCM is appiled in this study to investigate UHI and its impact on nighttime air chemistry

1. Introduction

2. Results

Figure 2 shows the simulated spatial distribution of skin temperature at 6:00 CST on July 18 and 25. The skin temperature over the urban area is higher than that over the surrounding area. The temperature difference between the urban and surrounding area (one measurement of urban heat island intensity) is more prominent on the night of July 17-18 than the night of July 24-25.

Figure 3 shows the temperature time series at six Oklahoma Mesonet sites and one portable weather information display system (PWIDS) deployed in the center of OKC. The model reproduced the temperature constrast between the urban and rural area on those two episodes. The urban heat island is prominent on the night of July 17-18 while it is negligible during the daytime. The urban heat island intensity on the night of July 24-25 is quite weak.

Figure 4 shows the potential temperature at the south-north cross section through OKC. At 6:00 CST on July 18, the potential temperature in the lower 200 m in the northern OKC is higher than the surrounding area. However on July 25, such phenomina is not prominent.

Figure 5 shows the vertical profiles of potential temperature at one urban and one rural sites. The temperature inversion near the surface on the night of July 17-18 is distinctly stronger than the night of July 24-25. The inversion near the surface (around 100 m) over urban on the night of July 17-18 is broken down due to stronger vertical mixing. Such stronger vertical mixing keep surface temperature from dropping significantly during the nighttime over urban. As a results the temperature near the surface over Urban is 1.5 ^{o}C higher that that over MINC. On the night of July 24-25, the near surface stability in the lower 500 m is weaker that the night of July 17-18. Under such environment, the contrast between the Urban and Rural area is not prominent.

Stability near the surface affects the dispersion of pollutants. Figure 6 shows the observed and simulated NOx near the surface. On the night of July 17-18, due to very strong inversion near the surface, vertical dispersion is depressed, thus more NOx is confined near the surface. On the night of July 24-25, NOx is dispersed to higher altitude due to weaker stability near the surface. Thus there is higher NOx mixing ratios on the night of July 17-18 than on the night of July 24-25. The model reprodueced NOx variation on those two night quite well, which implies that the model simulate the emission of NOx and meteorological variables near the surface quite well.

Figure 7 shows the spatial distribution of NOx. As explained above, due to weaker vertical dispersion on the night of July 17-18, NOx has higher mixing ratios on this night than that on the night of July 24-25 (Figure 8). Also we can notice that NOx is mostly confined in the area near the source, which indicates the lifetime of NOx is relatively short. It is also indicated that local emission is the dominant source of NOx and regional transport plays a minor role for NOx near the surface. On the contrary, O_3 has a longer lifetime and regional transport plays a more importrant role for contributing to ambient O_3. Thus O_3 may need longer spin-up time than NOx and approapriate boundary conditions are more important for O_3 simulation.

Figure 9 shows simulated and observed O_3 at six sites. Maximum O_3 on July 24 reachs ˜70 ppbv while it is around 40 ppbv on July 17. It is noticed that the temperature on

July 24 is lower than on July 17 (Figure 3). Higher temperature normally leads to higher local O_3 production. Lower O_3 on July 17 indicates regional transport also played an important role in determining the ambient O_3. The model reproduces the O_3 contrast on July 17 and 24, which indicates that the model reproduces regional transport and local production of O_3 quite well.

Figure 10 shows the simulated spatial distribution of potential temperature and wind field at ˜660m in domain 1 on the night of July 17-18 and July 24-25 to show the different regional transport on those two nights. on the night of July 24-25, cooler continental air mass moved in Oklahoma from the southeast while on the night of July 17-18 warmer air mass moved in from the southwest. This explains the higher potential temperature at the altitude of 0.5-1 km on the night of July 17-18 comparing to that on the night of July 24-25 (Figure 5). As a result, the inversion below 0.5 km on the night of July 17-18 is stronger.

Different air masses have different concentraions of pollutants. Figure 11 shows the O_3 mixing ratios at ˜660m. On the night of July 24-25, continental air mass from the east contains more O_3 moved in Oklahoma while the air mass from the southwest on the night of July 17-18 is cleaner. Such different regional transport played an important role in dictating the different O_3 levels on those two episodes

Different regional transport of O_3 is reflected in the vertical profiles of O_3 shown in Figure 12. The O_3 in the residual layer (0.5-1.2km) on the night of July 17-18 is much lower than that on July 24-25. Different stability near the surface also affected the O_3 profile near the surface. O_3 is removed near the surface due to NO titration and dry deposition near the surface. Strong stability near the surface on the night of July 17-18 suppressed vertical mixing of O_3, thus O_3 shows strong gradient near the surface (below 500 m) on the night of July 17-18. However on the night of July 24-25, O_3 in the lower 500m is more mixed.

Urban heat island impacts of surface O_3 and NOx. In the Northern OKC, where urban heat island is most prominent, more regorious vertical mixing increased surface O_3 on the night of July 17-18 (Figure 13). Thus the contrast of O_3 between Norther OKC and the surrounding area is more prominent than that on the night of July 24-25.

The profiles of O_3 in the center of UHI and the surrounding rural area is displayed in Figure 14. The O_3 in the lower 200 m is increased by 2-3 ppbv due to the UHI effect.

Acknowledgments. TACC ranger

References

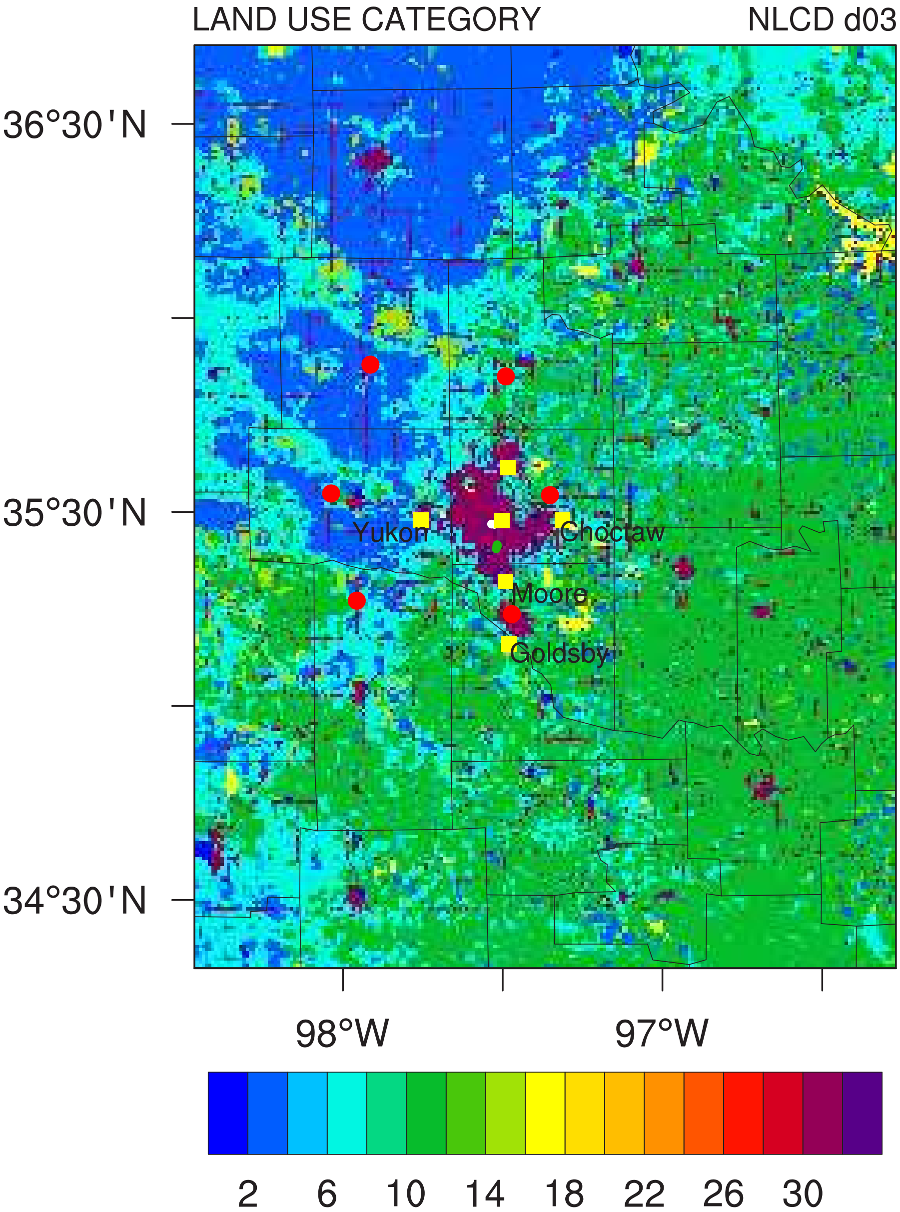

Figure 1. Land use categories in domain 3, yellow squares shows the location of air quality monitoring sites and red circles shows the location of Mesonet sites

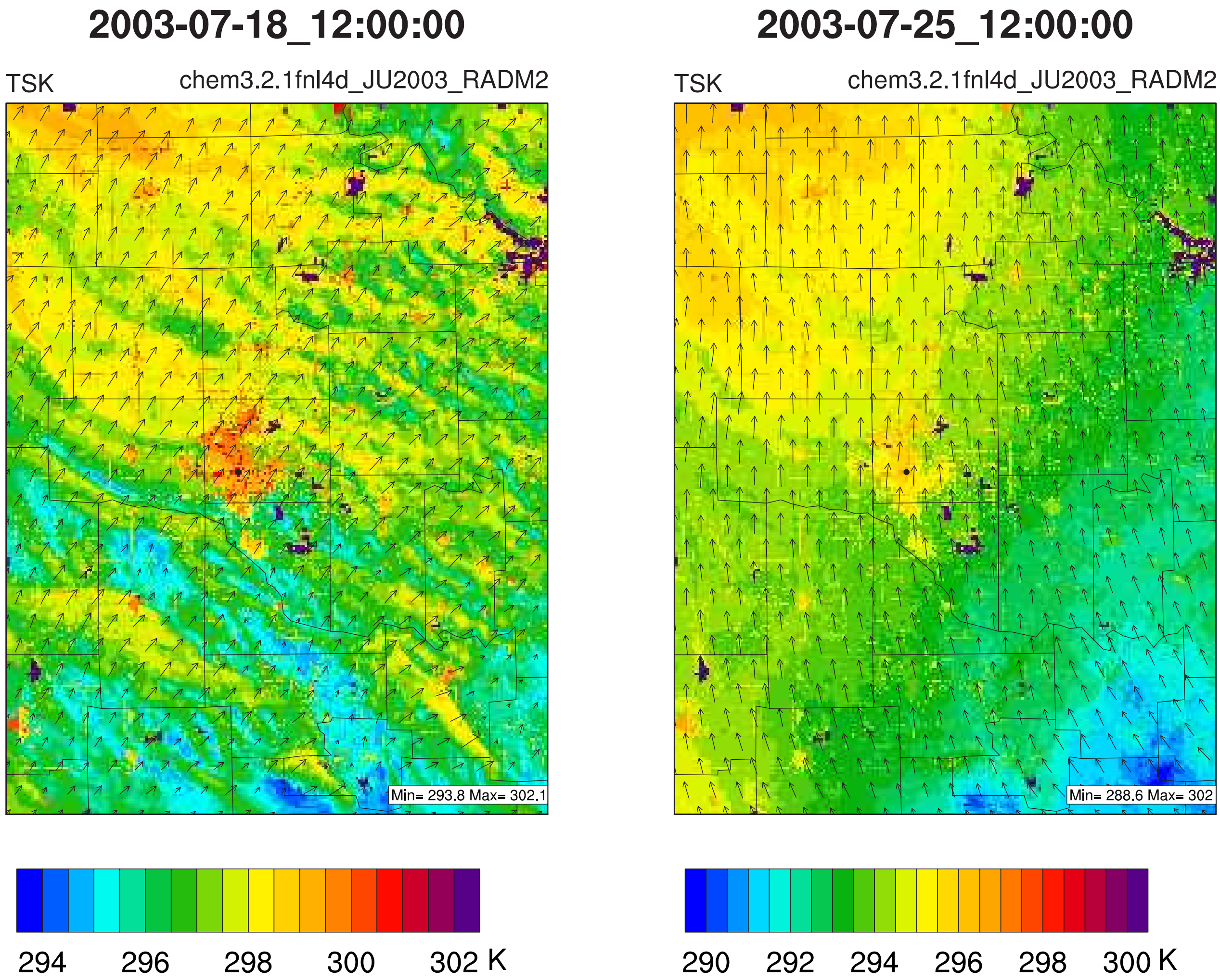

Figure 2. Simulated spatial distribution of skin temperature

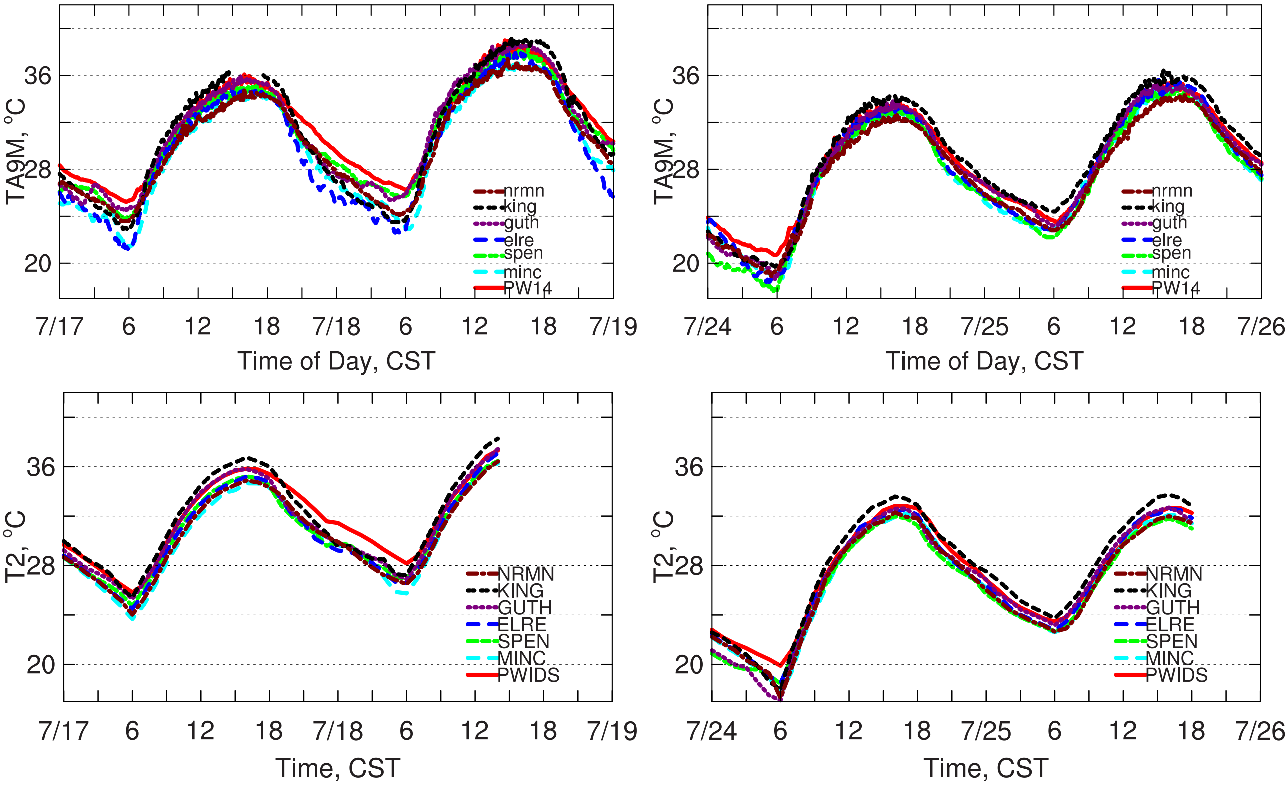

Figure 3. (Top) Observed and (Bottom) simulated time series of temperature

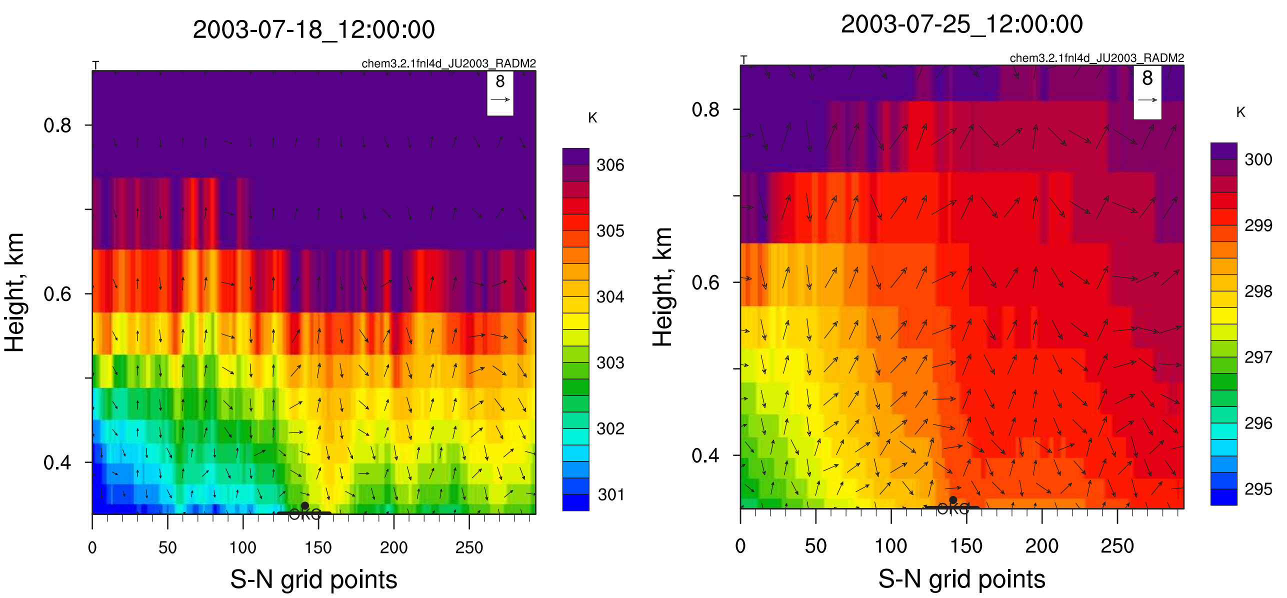

Figure 4. Simulated potential temperature at S-N cross-section through OKC

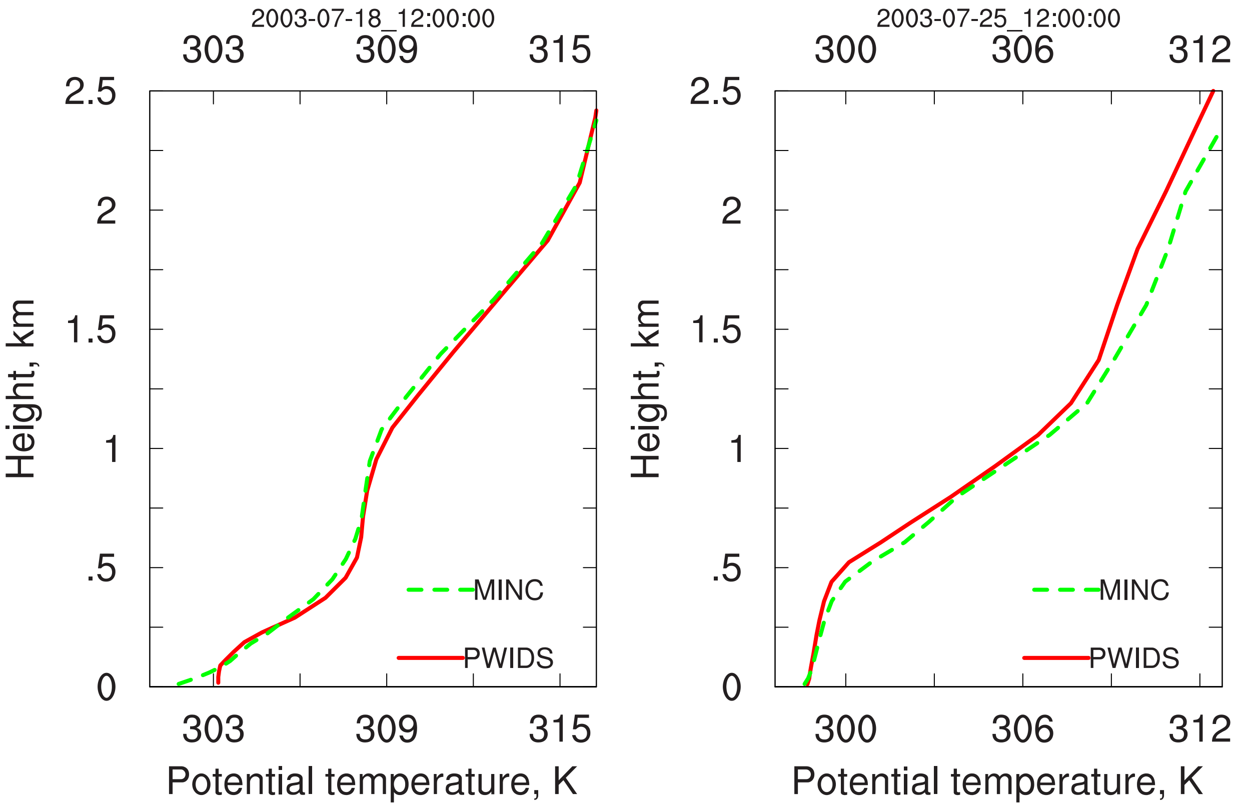

Figure 5. Simulated profiles of potential temperature

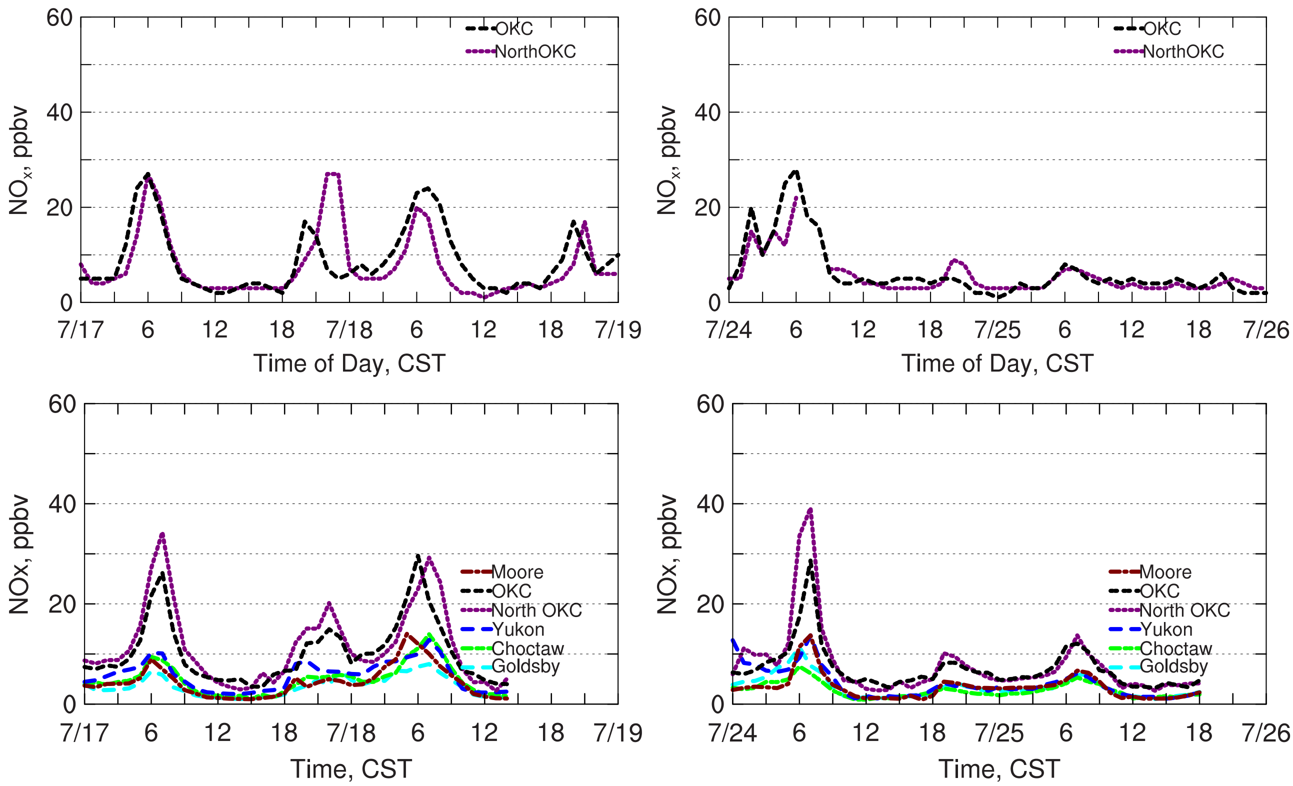

Figure 6. (Top) Observed and (Bottom) simulated time series of NOx

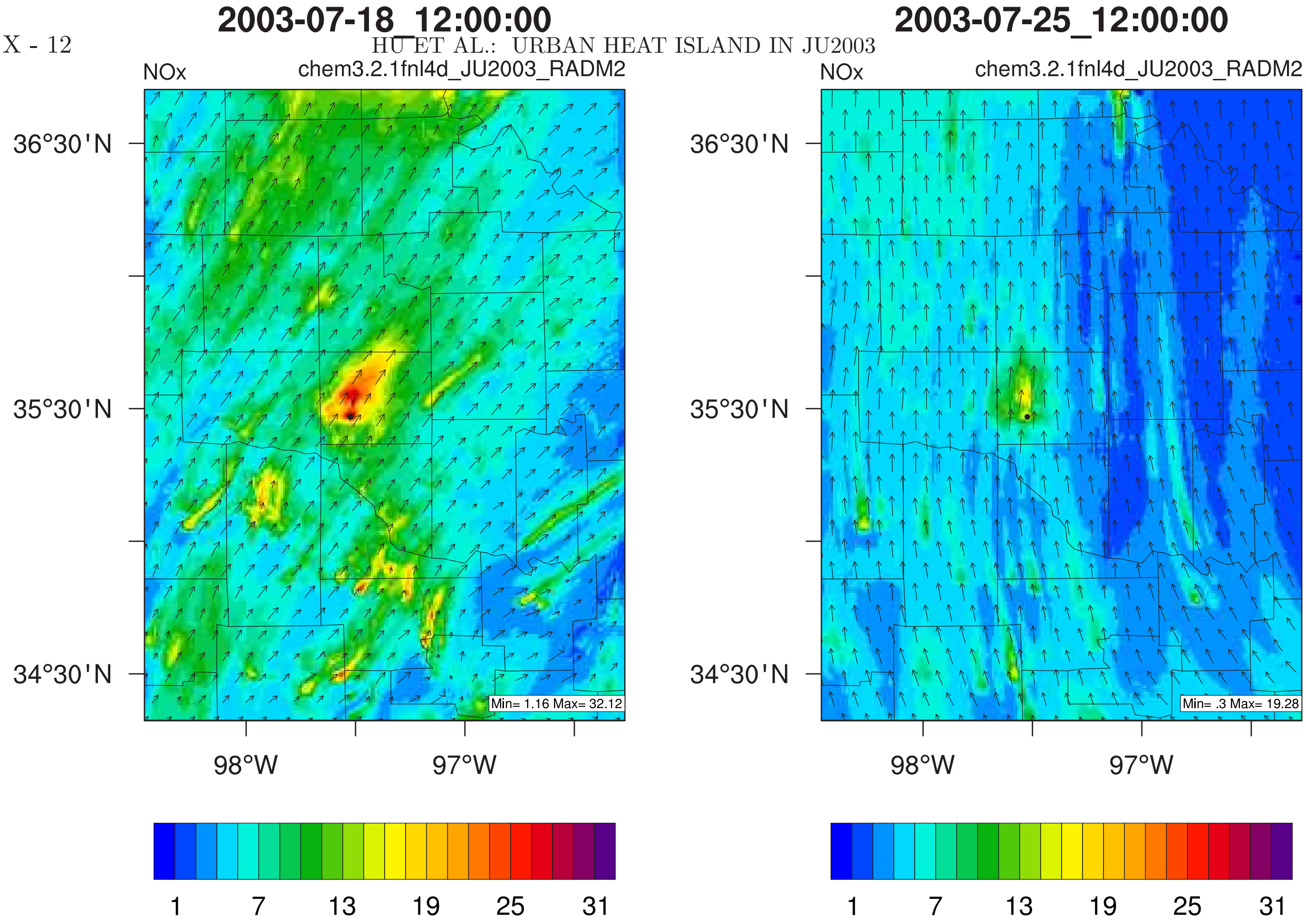

Figure 7. Simulated NOx spatial distribution

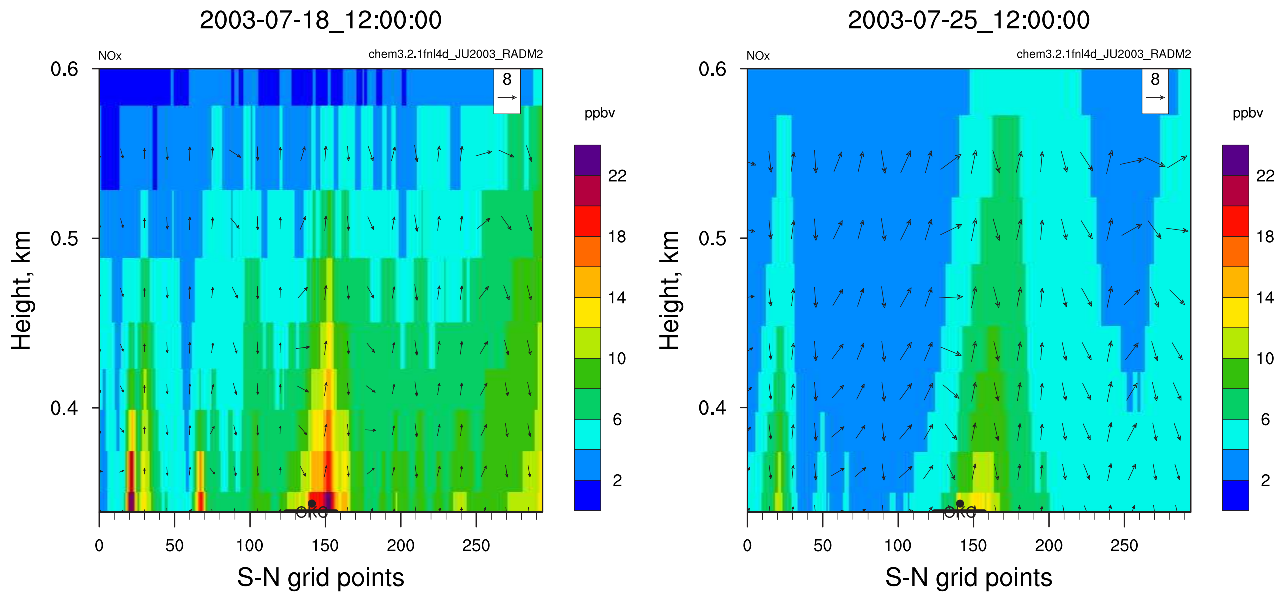

Figure 8. Simulated NOx at S-N cross-section through OKC

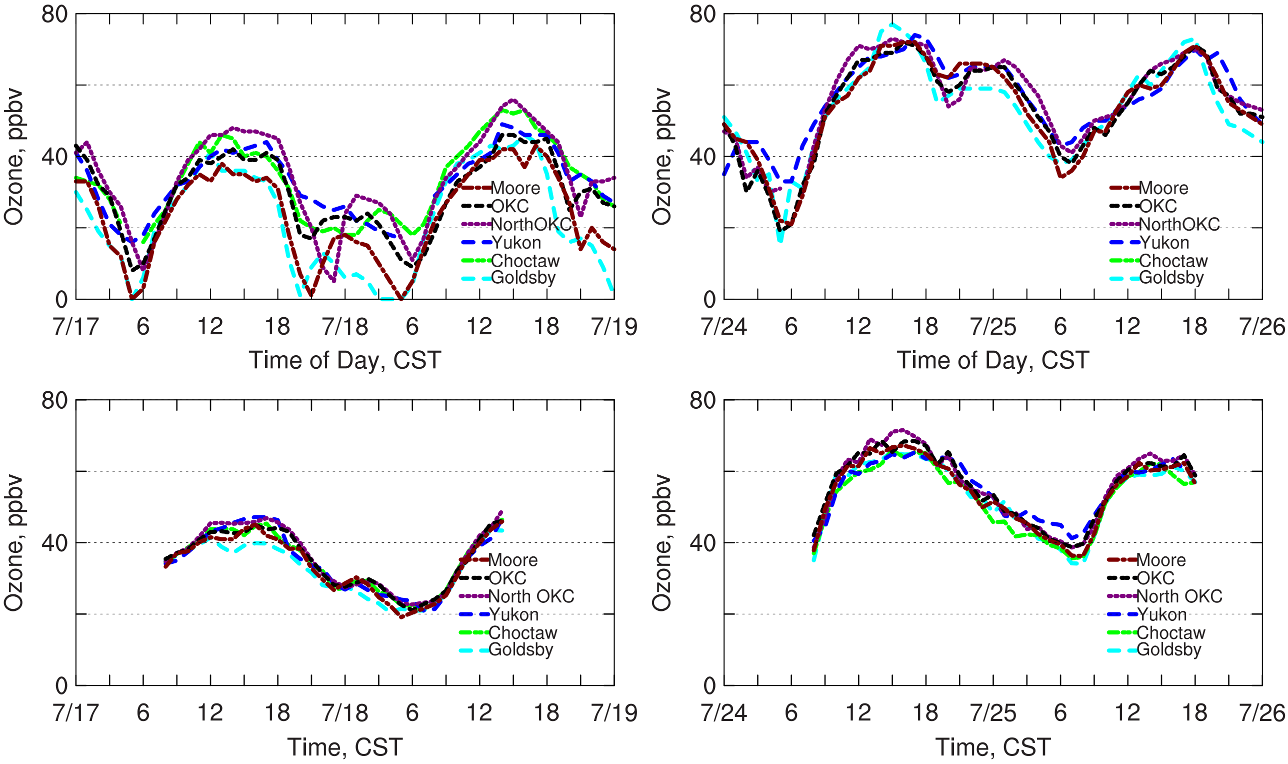

Figure 9. (Top) Observed and (Bottom) simulated time series of ozone

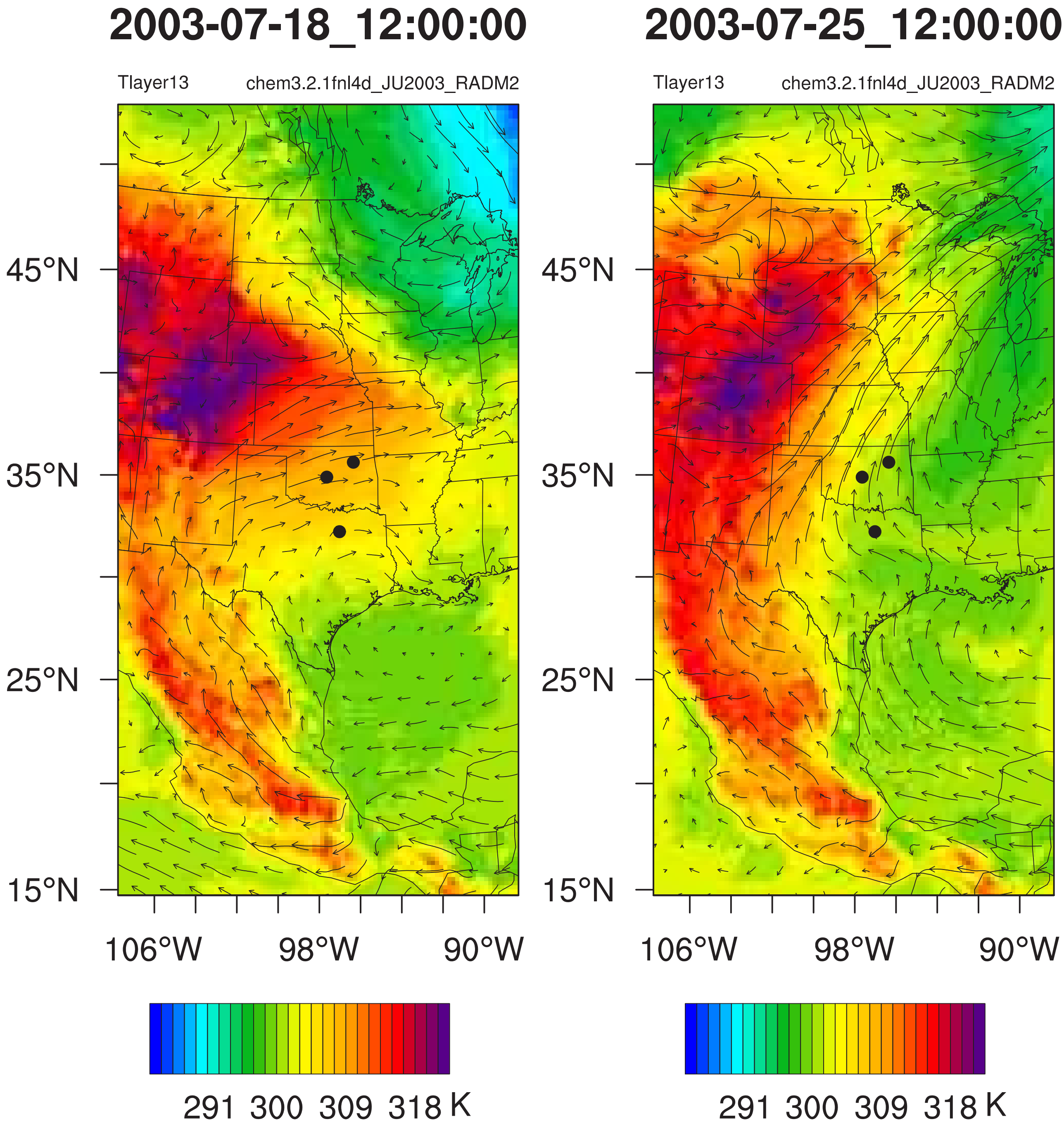

Figure 10. Simulated spatial distribution of potential temperature at ~660m

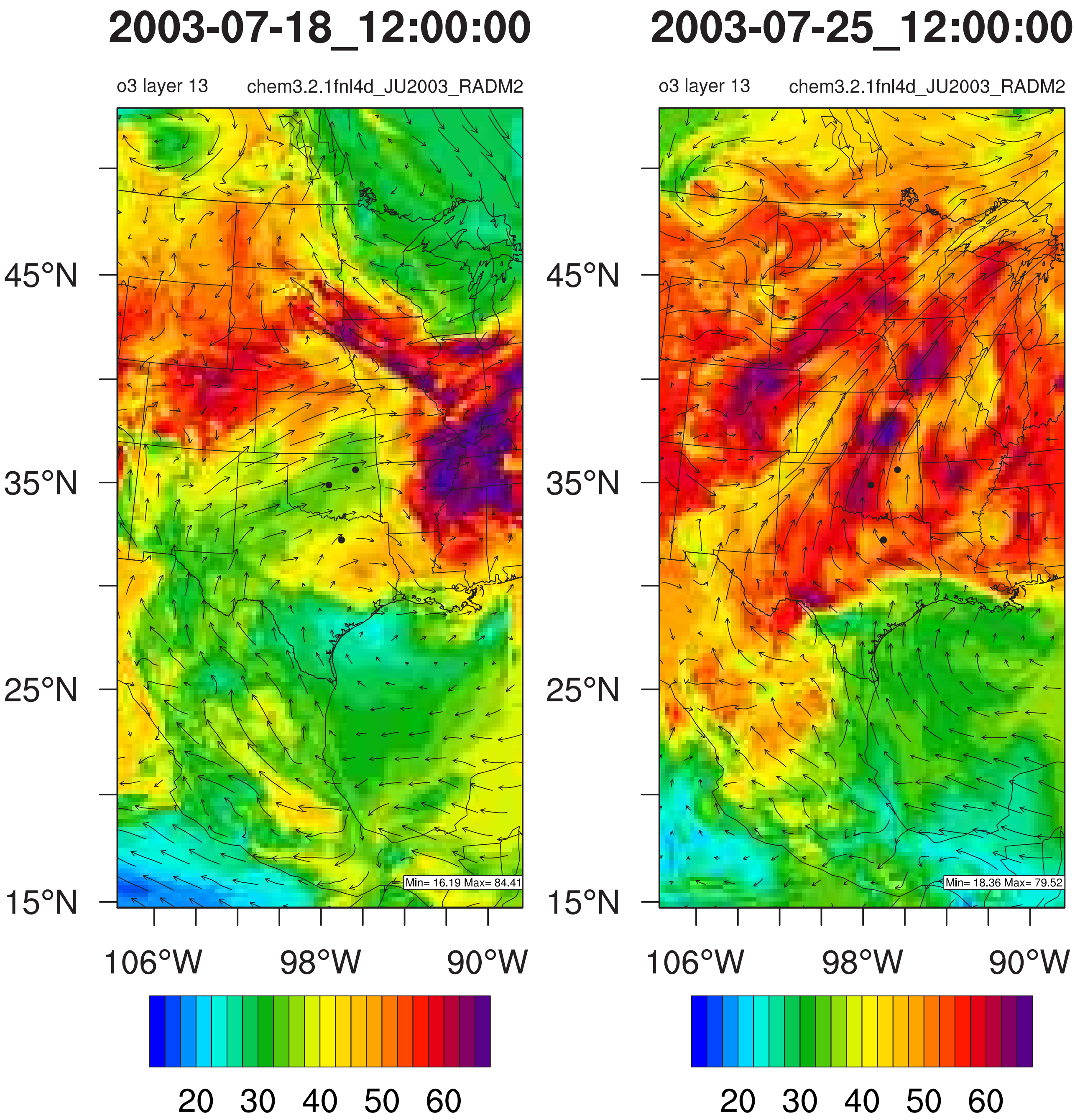

Figure 11. Simulated ozone spatial distribution at ˜660m

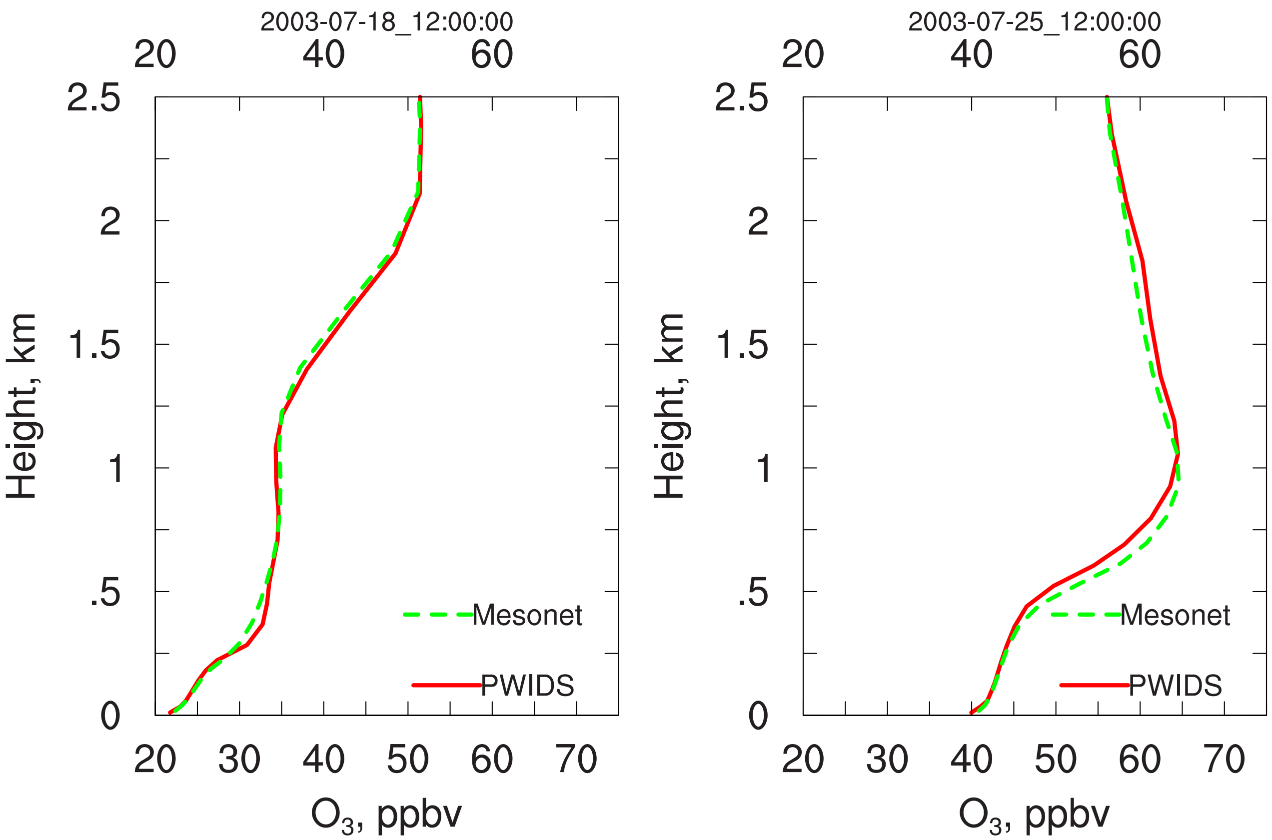

Figure 12. Simulated ozone profiles

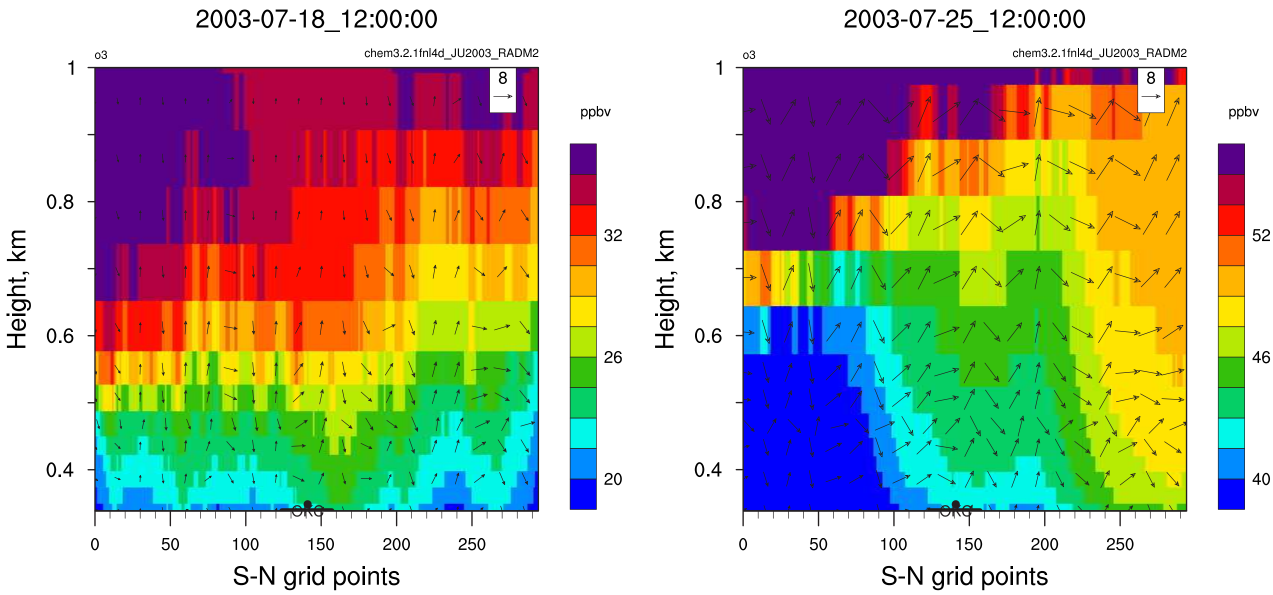

Figure 13. Simulated O_3 at S-N cross-section through OKC

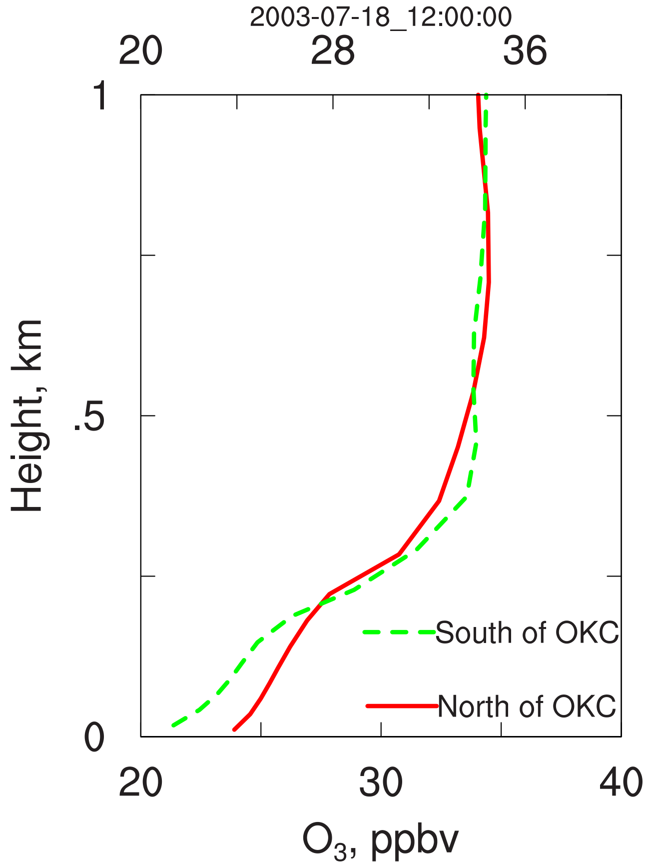

Figure 14. Profiles of O_3 at North of OKC (center of UHI) and South of OKC